Preliminary Analysis of Fluctuations in the Received Uplink-Beacon-Power Data Obtained From the GOLD Experiments

M. Jeganathan, K. E. Wilson, and J. R. Lesh
Communications Systems and Research Section

Uplink data from recent free-space optical communication experiments carried out between the Table Mountain Facility and the Japanese Engineering Test Satellite are used to study fluctuations caused by beam propagation through the atmosphere. The influence of atmospheric scintillation, beam wander and jitter, and multiple uplink beams on the statistics of power received by the satellite is analyzed and compared to experimental data. Preliminary analysis indicates the received signal obeys an approximate lognormal distribution, as predicted by the weak-turbulence model, but further characterization of other sources of fluctuations is necessary for accurate link predictions.

I. Introduction

An optical communication link between an Earth-orbiting satellite and a ground-based receiver involves propagation of a laser beam through the atmosphere. Spatial and temporal variations in the index of refraction of the air that forms the atmosphere severely degrade the quality of the beam. These variations, typically lasting on the order of one thousandth of a second at optical and near-infrared (NIR) frequencies, in the index of refraction result in random changes in the amplitude and phase of the arriving wave. The amplitude and phase fluctuations manifest themselves in effects such as scintillation, beam broadening, and beam motion or wander. Scintillation can be thought of as interference between partial waves propagating through different paths (or turbulent cells), which results in fades (destructive interference) or surges (constructive interference) at the receiver. Deep fades causing signal loss or strong surges causing saturation of the quad-detector can force loss of track. On the uplink, with the exception of heavy cloud cover, atmospheric scintillation is usually the limiting factor in an optical link. For downlink, however, the large size of the receiver's aperture typically compensates for scintillation by averaging over fades and surges. Beam motion, primarily on the uplink, can often be considered as atmospheric-induced jitter in the pointing of the laser beam. Such motion of narrow beams can cause deep fades in the signal due to the Gaussian nature of the spatial beam profile.

In this article, we use data from the recent Ground/Orbiter Lasercomm Demonstration (GOLD) experiments to study the atmosphere-induced fluctuations in signal power on the uplink. The experiment's objective is to establish a 1-Mbps optical communication link between the laser communication experiment (LCE) package on board the Japanese Engineering Test Satellite (ETS-VI) and the Table Mountain Facility (TMF) near the Jet Propulsion Laboratory (JPL). The link is established by first transmitting a

beacon from TMF to ETS-VI using a priori knowledge of the satellite's orbit. The beacon is subsequently acquired and tracked by the LCE package on the satellite. Once the tracking loop is activated on the LCE, an onboard laser is turned on for downlink. The downlink beam is then picked up by the receiver at TMF to complete the link. Once the link is established, both the downlink laser and uplink beacon can be modulated for transmission of data. Here, we shall restrict our analysis to scintillation-induced signal fluctuations on uplink and ignore the communication aspect of the experiment.

In the following analysis, we compare the statistics of the power received by the detectors on board the satellite when a continuous wave (CW) beacon is transmitted from TMF to the probability distribution function (pdf) predicted by existing models for atmospheric propagation. In Section II, we begin with a brief summary of the theory that takes into account atmospheric scintillation, jitter, and multiple uplink beams. Section III provides the specifics of the experiments and a typical link budget for the uplink. The experimental data are presented in Section IV. The final section discusses the observed results in comparison with theoretical predictions and offers potential sources of discrepancy between the theory and the experiment.

II. Theory

Consider a communication channel between a ground station and an orbiting satellite that is specific to GOLD, as shown in Fig. 1. A detailed discussion of the influence of the atmosphere on the statistics of the channel during beacon uplink follows. Figure 2 shows a system-level representation of the optical channel. We will show that the power, P_R, received by the photodetector on the satellite is the product of three quantities:

$$P_R = P_0 I S$$

where P_0 is the power received in the absence of a turbulent atmosphere, I is a random variable with a beta-distribution caused by atmospheric and pointing jitter, and S typically is a lognormal random variable due to scintillation. The maximum receivable power, P_0, at the satellite is assumed to have zero variance. Thus, fluctuations due to the laser and detector noise are assumed to be negligible compared to scintillation and beam jitter. In the following sections, the major contributions to the observed statistics of the received power are described.

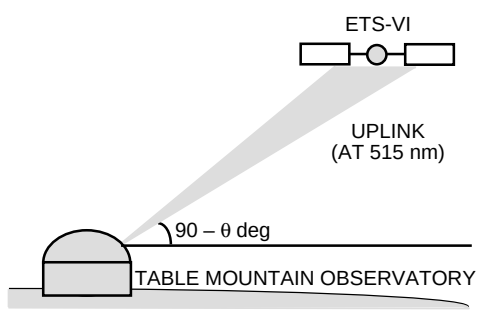

Fig. 1. Geometry of a ground-to-orbiter laser communication link showing transmission from TMF to ETS-VI.

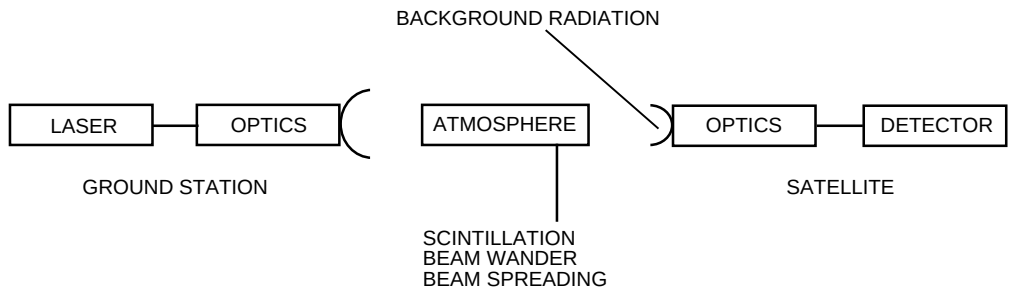

Fig. 2. Components and channels in an optical communication system.

A. Free-Space Propagation

For an optical transmitter with continuous wave (CW) laser power of P_T W, the power received by the detector on board the satellite in the absence of atmospheric turbulence is primarily governed by free-space-propagation loss and optical absorption. Taking into account optical losses at the transmitter and receiver and atmospheric absorption, we find that the received power is given by

$$P_0 = \eta_{roe}\eta_{toe}\eta_0^{\sec\theta}\frac{4}{\pi}\frac{A_R P_T}{(Z\Theta_{bd})^2}$$

where Z is the communication range in meters; Θ_{bd} is the laser beam divergence in radians; θ is the zenith angle to the receiver looking from the transmitter station; η_{toe} is the transmitter optical efficiency; η_{roe} is the receiver optical efficiency; η_0 is the atmospheric transmission at zenith; and A_R is the area of the receiver's aperture in square meters. The exponent $\sec\theta$ is often referred to as the air mass. We may to a good approximation assume that all quantities in the above equation are constant over the duration of the experiment, which typically lasts a few hours.

B. Light Wave Propagation in Turbulent and Random Media

Wave propagation through lossless random media, like the atmosphere, is often characterized by the structure constant C_n^2, which is a measure of the variance of the index of refraction, n, due to inhomogeneities in the medium [1]. For modeling the atmosphere, one often needs to know the altitude variation of the structure constant and its dependence on weather conditions. Though modeling the atmosphere is a difficult task, there exist several empirical and parametric models for the altitude variation in the structure constant of the atmosphere. The most common of these is the theoretically based Hufnagel model, in which the dominant turbulence arises from winds in the 5- to 20-km altitude range [2]. The altitude of TMF (2.2 km above sea level) is well outside the range of validity of the Hufnagel model (over 5-km above sea level). The validity of the improved Hufnagel–Valley model [3], on the other hand, extends down to the ground. This model, however, predicts a larger than observed turbulence at TMF by overestimating the low-altitude contribution. We, therefore, use the experimentally based Air Force Geophysical Laboratory (AFGL) CLEAR I night model [4]. The AFGL CLEAR I night model is based on the average of a large number of measurements of the atmospheric properties in the New Mexico Desert. The model provides the functional dependence of C_n^2 on altitude down to 1.23 km above mean sea level:

$$\log_{10} C_n^2 = A + Bh + Ch^2 + D\exp\left\{-0.5\left[\frac{h-E}{F}\right]^2\right\}$$

where h is the altitude in km above mean sea level. The constants A, B, C, D, E, and F are defined for three different ranges of altitude and listed in Chapter 2 of [3]. Most quantities of interest are usually expressed as weighted integrals of the index of refraction structure constant, as described below.

Consider, for example, observation of a star with a large aperture telescope. As noted earlier, the large aperture negates the effect of scintillation by averaging over constructive and destructive interferences. Since light from a distant object can be well approximated by plane waves, the only prominent effect of the turbulent atmosphere is thus the change in the angle of arrival of the plane wave. The random arrival angle limits the resolution of the telescope. In fact, the resolution of the telescope is equivalent to the resolution of an aperture, r_0 (called the coherence length of the atmosphere), determined by the atmospheric structure constant and wavelength of light [5]:

$$r_0 = \left[0.42k^2 \sec\theta \int_{h_0}^{Z} C_n^2(h)dh \right]^{-3/5}$$

where k is the wave vector $(2\pi/\lambda)$ of the plane wave; h is the height above sea level; and h_0 is the altitude of the location of the telescope. From basic principles of optics, an aperture with diameter r_0 has a full-width-half-maximum (FWHM) angular resolution of

$$angular\ resolution\ = \frac{\lambda}{r_0}$$

For a wavelength of 0.5 μm, the coherence length r_0 is on the order of 10 cm. In experimental observations, it is convenient to define "seeing" as the FWHM of the angular spread of the star. For r_0 of 10 cm, the seeing is approximately 1 arcsec, or 5 μrad. It must be noted that though subarcsecond seeing conditions are possible at TMF, a more representative value for the seeing at TMF is 2–3 arcsec, or an r_0 of a little under 5 cm.

Given the AFGL CLEAR I model for the altitude dependence of the structure constant, the above equation for r_0 gives a single value for the atmospheric coherence length irrespective of the meteorological conditions. To better model the existing local weather conditions, we scale the structure constant function by a multiplicative constant so that the predicted value of r_0 matches the r_0 derived from measured seeing. The scaled C_n^2 is then used to determine other atmospheric-related quantities, such as scintillation variation and beam wander. For this purpose, the seeing was measured several times during a single run of the GOLD experiment.

C. Beam Motion and Jitter

To account for intensity fluctuations due to pointing inaccuracies and beam wander, we assume a Gaussian intensity profile for the uplink laser beam. That is, the normalized intensity pattern takes the form

$$I\left(\delta_x, \delta_y\right) = \exp\left[-4 \left(\frac{\delta_x + \delta_y}{\Theta_{bd}} \right)^2 \right]$$

where δ_x and δ_y are the angular deviation or error in the pointing. If the transmitter and receiver are on-axis and there is no pointing offset ($\delta_x = \delta_y = 0$), the receiver would see a power P_0 from the transmitter. Because of pointing jitter and atmospheric-induced beam motion, however, δ_x and δ_y are random variables (RVs) and not constants. We assume δ_x and δ_y to be identically and normally distributed with zero mean and variance σ_j^2. The variance σ_j^2 is the sum of the variance of atmospheric-induced and transmitter-induced pointing errors. The variance of the atmospheric-induced beam motion is again given by a weighted integral of the structure constant [5, Chapter 6], but as a first-order approximation, we assume it to be equal to the seeing. The transmitter-induced jitter is more difficult to ascertain, but is typically small relative to atmospheric effects.

The new random variable I can be shown to have the following cumulative probability distribution function (CDF) [6]:

$$P_I(I \leq i) = F_I(i) = i^{\beta} \quad \text{for} \quad 0 < i < 1$$

where

$$\beta = \frac{1}{8}\left(\frac{\Theta_{bd}}{\sigma_j}\right)^2$$

is a measure of the pointing accuracy with respect to the beamwidth. We immediately see that the mean and variance of I are given by

$$< I >= \frac{\beta}{\beta + 1}$$

and

$$< I^2 > - < I >^2 = \frac{\beta}{(\beta+1)^2} \; \frac{1}{\beta + 2}$$

respectively. It is obvious that a large value of β is desirable. In fact, for large values of β, the mean approaches the optimum value of 1 and the variance tends to 0 as $1/\beta^2$. For small values of $\beta, (\beta << 1)$, on the other hand, both the mean and variance are proportional to β.

To achieve a large value of β, either the angular beamwidth must be increased or the beam jitter must be decreased. With little control over the atmospheric-turbulence-induced beam wander, one is often limited in practice to increasing the beam divergence for obtaining a particular value of β. But the received power is inversely proportional to the square of the beam divergence. An optimum value of β, therefore, exists and depends on atmospheric conditions. The statistical analysis of the effect of a constant pointing offset is complicated by the loss of circular symmetry, and one may be forced to resort to numerical or Monte-Carlo simulations for a complete analysis. Thus, for simplicity, we will account for constant pointing offset only through an exponential loss factor, which is a reasonable assumption if the offset is much smaller than the beam divergence.

D. Atmospheric Scintillation

The pdf of the normalized received intensity, S, at a point receiver due to scintillation can take several forms. For weak turbulence, the pdf takes on a lognormal distribution. This can be understood from the fact that S is proportional to

$$S \propto |\exp(\chi + i\phi)|^2$$

where χ and ϕ are the amplitude and phase of the wave, respectively, and both are normally distributed random variables. The quantity 2χ is often referred to as the log-irradiance. For strong turbulence over long paths, the intensity fluctuations are severe and the distribution is exponential. Andrews and Phillips have shown that the scintillation takes the form of an I-K (i.e., containing I and K Bessel functions) distribution, which reduces to the two limits given above for weak and strong turbulence [7,8]. Since the GOLD experiments were performed at a relatively high altitude (2.2 km for TMF) and the source of most

turbulence is at or near sea level, we assume a weak turbulence model and use the lognormal distribution for S. That is,

$$f_S(s) = \frac{1}{\sqrt{2\pi\sigma_l^2}} \frac{1}{s} \exp\left[-\frac{1}{2\sigma_l^2} \ (\ln s - l_m)^2\right]$$

where $l_m = -\sigma_l^2/2$ is the mean of the log-irradiance distribution. The S, being a normalized quantity, has a mean of 1. The variance of the log-irradiance is determined from the following weighted integral of the index of refraction structure constant [9,10]:

$$\sigma_l^2 = 2.24k^{7/6} \ (\sec\ \theta)^{11/6} \int_{h_0}^{Z} C_n^2(h) h^{5/6} \ dh$$

where k, h, and h_0 are as defined before. Experiments have shown that σ_l^2 does not arbitrarily increase with increasing atmospheric turbulence [11]. In fact, the scintillation variance reaches a saturation value of approximately $0.25\sigma_l^2 = 0.3$ and even decreases for high levels of turbulence. The variance of S itself is given by

$$\sigma_S^2 = \exp(\sigma_l^2) - 1$$

Note that it is customary to characterize the lognormal distribution of S using the mean and variance of the log-irradiance. Thus, neither the mean nor the variance of S is immediately apparent from $f_S(s)$. Given $y = \exp(x)$, where x is a Gaussian RV, and thus y is a lognormal RV, we use the following convention: By log-variance of y, we mean the variance of x.

Combining the effect of atmospheric scintillation and beam-pointing errors, the received power can be written as

$$P_R = \eta_{toe}\eta_{toe}\eta_0^{\sec\theta} \frac{4}{\pi} \ \frac{A_R P_T}{(Z\Theta_{bd})^2} IS$$

We emphasize that in the above equation I and S are RVs. The pdf of the received signal resulting from the product of a lognormal and beta-distributed random variable can be derived analytically. This, however, involves the use of cumbersome integral functions. Through Monte-Carlo simulations, Kiasaleh has shown that, for a scintillation variance larger than 0.2, the pdf of the product of S and I can be approximated by a lognormal distribution [12]. We will, therefore, assume the received power P_R to be lognormally distributed to arrive at an analytical expression for the final result.

The voltage readout, V, of the detection system on board the satellite is the product of the received power and the transimpedance gain, G, of the detector–amplifier combination. That is, $V = G\ P_R$. In principle, the statistics of the detector and amplifier must be taken into account for accurate analysis. For the case at hand, scintillation and jitter are dominant, and we therefore assume the statistics of V to be identical to P_R. The pdf of V, being lognormal, is

$$f_V(\nu) = \frac{1}{\sqrt{2\pi\sigma^2}} \frac{1}{\nu} \exp\left[-\frac{1}{2\sigma^2} (\ln\nu - \ln\nu_0)^2\right]$$

To determine the value of ν_0 and σ, we use the properties of independent RVs. That is, $\langle V \rangle = GP_0 \langle I \rangle \langle S \rangle$ and $\langle V^2 \rangle = (GP_0)^2 \langle I^2 \rangle \langle S^2 \rangle$. Moreover, from the properties of the lognormal distribution, $\ln \nu_0 = -0.5\sigma^2 + \ln\langle V \rangle$ and $\sigma^2 = \ln\langle V^2 \rangle - \ln\langle V \rangle^2$. From these expressions, we find that

$$\sigma^2 = \sigma_l^2 + \ln \frac{(1+\beta)^2}{(2+\beta)\beta}$$

and

$$\ln \nu_0 = \ln [GP_0] - \frac{1}{2}\sigma_l^2 - \frac{1}{2} \ln \frac{(1+\beta)^3}{(2+\beta)\beta^2}$$

The photodetector/amplifier gain factor G has units of volts per watt. The mean and variance of the received signal are not independent, as they both depend on β and σ_l^2. For example, an increase in atmospheric turbulence resulting in a larger scintillation variance will decrease the mean.

E. Effect of Multiple Uplink Beams

The adverse effect of scintillation can be reduced by the use of multiple uplink beams, each incoherent with the rest and separated by a distance larger than the atmospheric coherence diameter, r_0. For such a case, the signal arriving at the detector is the sum of the signal from each uplink beam with independent identically distributed (i.i.d.) statistics. That is,

$$S = \frac{1}{N} \sum_{n=1}^{N} S_n$$

where N is the number of independent beams, and the random variables S_n are lognormally distributed. We assume that the total uplink power remains constant and, thus, each beam has $1/N$th of total power. From the properties of sums of i.i.d. random variables, we find that S is a convolution of N lognormal distributions. Analytic expressions for the convolution of lognormal functions are unavailable, and thus we resort to numerical techniques using characteristic functions and fast Fourier transforms (FFTs). Note that for a large N, according to the central limit theorem (CLT), the distribution of S approaches a Gaussian.

To illustrate the benefits of launching multiple beams during uplink, we choose, as an example, a mean of $100/N$ and a log-variance of 0.6 for each S_n. Figure 3 shows the expected pdf when total laser power is equally distributed in 1, 2, 4, 8, or 16 beams. Several features are worth noting. First, the means for all the distributions are the same. Second, the location of the peak of the pdf approaches the mean of S when N is increased. Finally, the pdf is concentrated around the mean for large values of N. In short, though the mean varies little with an increasing number of beams, the variance drops significantly with additional beams. In fact, for the example in the figure, the standard deviations are 88, 64, 45, 32, and 23 for 1, 2, 4, 8, and 16 beams, respectively. That is, the standard deviation is approximately one-half with 4 beams and one-quarter with 16 beams.

In the presence of strong scintillation, dividing the laser power into several beams is essential for avoiding deep fades and surges. The number of beams needed to achieve a given bit-error rate (BER) will depend on the strength of the scintillation. One can, in principle, increase the number of beams arbitrarily to improve signal statistics at the receiver. Practical considerations, such as efficiency of dividing the laser power, modulation timing accuracy, and, most importantly, the available space, however, will typically limit the number of beams to less than 10.

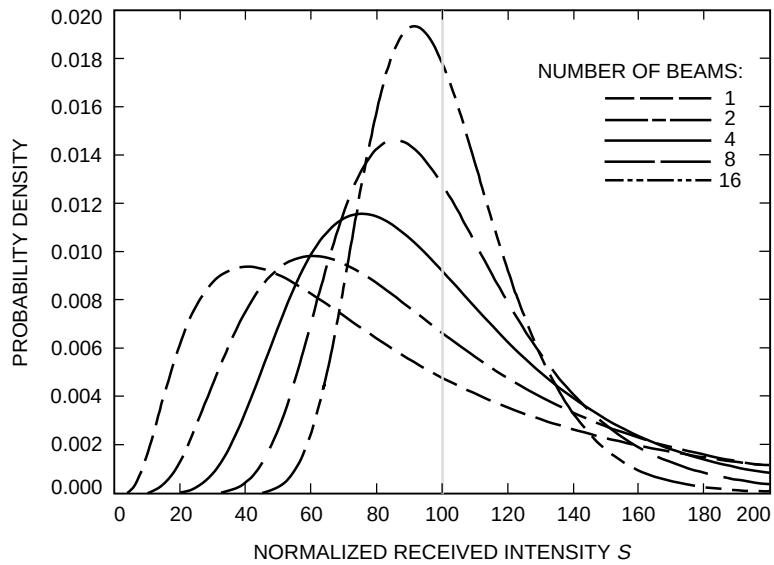

Fig. 3. The pdf of the received signal intensity, *S*, showing the improvement in variance with multiple uplink beams.

Part of the objective of GOLD is to understand the effects of multibeam propagation through the atmosphere. In the GOLD experiments, light from the laser is split into two and the path length of one of the beams is increased by a distance greater than the coherence length of the laser. The two beams are then launched into the coudé so as to emerge from the primary separated by a distance of 20 cm (which is much greater than r_0). Thus, the actual variance of the received signal will be less than that predicted by the single-beam model.

III. Link Budget

Table 1 shows the link budget for transmission of a single high-power CW beam from TMF up to the satellite on November 17, 1995. The link budget is for the quad-photodetector (QPD) on the satellite. All data concerning the laser communication package on the satellite are provided by the Communication Research Laboratory (CRL) in Japan. Parameters pertaining to the TMF transmitter were determined experimentally. Atmospheric-related parameters were estimated from "seeing" conditions, as described earlier. We assume that the beam wander is dominated by atmospheric-induced motion and that it is equal to the seeing. Finally, background radiation from Earth reaching the detector is negligible, as the experiments are conducted at night from TMF. Values of parameters such as range, elevation, and seeing represent average values for the duration of the experiment. The atmospheric scintillation contribution to the log-variance is 0.52 in the above calculation. The remainder of the contribution to the variance is from atmosphere-induced beam wander. The effect of two beams on the expected variance is discussed in the next section.

IV. Experimental Data and Analysis

Figure 4 shows the QPD signal versus time for an approximately 100-min time period when two CW beams (each with ∼6.6 W of power) were sent up to the satellite. The data were collected on the 17th of November 1995. The QPD signal was sampled every second and sent down through RF telemetry. Furthermore, the QPD has a gain value of 0.22 V/nW in the "low" gain setting, a gain value of 4.60 V/nW in the "high" gain setting, and few other intermediate settings. During the time corresponding to Fig. 4, the gain was set to low. Figure 5 shows the histogram of the signal shown in Fig. 4. The most likely

Table 1. Link budget for a single beacon uplink from TMF to ETS-VI.

Parameter	Value	Equivalent value, dB/dBm
Range (satellite to TMF distance)	37,850 km	—
Zenith angle	43.8 deg	—
Seeing	6 μrad	—
Transmitter information		
Laser wavelength	514.5 nm	—
Laser power	13,200 mW	41.21 dBm
Optical transmission[a]	0.75	−2.22 dB
Beam divergence	20 μrad	—
Pointing loss	4 μrad	−0.09 dB
Pointing jitter	0 μrad	—
Free space/atmosphere		
Propagation loss	—	−56.53 dB
Estimated atmospheric transmission at zenith	0.80	—
Atmospheric loss (at zenith angle)	—	−1.34 dB
Receiver information		
Aperture diameter	7.50-cm	−23.55 dB
Optical transmission	0.15	−8.24 dB
Received power (no turbulence)	10.49 nW	−49.79 dBm
Sensitivity ("high" gain)	631.0 pW	−62.00 dBm
Margin	16.62	12.21 dB
Reduction due to scintillation	0.77	−1.11 dB
Reduction due to jitter	0.71	−1.48 dB
New received power	5.7 nW	−52.38 dBm
New margin	9.0	8.89 dB
Net log-variance, σ^2	0.69	—
Probability of detection with above sensitivity	99.6 percent	—
Scintillation fades greater than 3 dB	33.7 percent	—

[a] Estimate based on losses in optical train components and reflectivity of telescope mirrors.

value of the QPD signal was approximately 1.2 V. The clustering of points around the maximum value of 4.5 V indicates saturation of the detector due to scintillation-induced surges, while clustering near the minimum value of 0 V indicates the beam was outside the field of view of the QPD due to tracking errors. The fact that the statistics of the received signal are not lognormal but rather a convolution of two lognormal distributions makes analyzing the data difficult because of the lack of an analytic expression for the convolution. The histogram data may nonetheless be fit to a lognormal function to obtain an approximate value for the mean and log-variance. To do so, the histogram data were fit to a scaled lognormal distribution, $A\ f(\nu)$, in an indirect way. The lognormal distribution can be written as a second-order polynomial by appropriate transformation of variables. Let $w = \ln f(\nu)$ and $u = \ln \nu$. By taking the log of the lognormal distribution function, we have

$$w = au^2 + bu + c$$

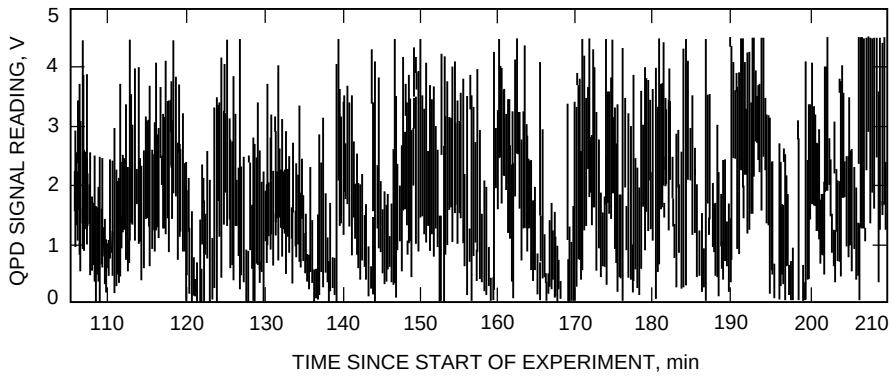

Fig. 4. The QPD signal reading versus time in minutes since the start of the experiment (10:40 UTC) on November 17, 1995.

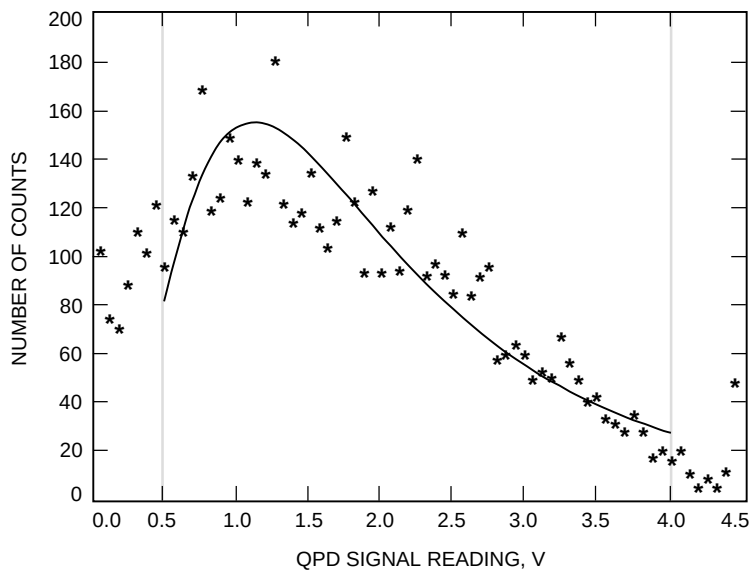

Fig. 5. Histograms of the QPD signal reading. The asterisks show the number of times a given signal level was observed in the time interval of interest. The solid line is a fit of the histogram data to a log-normal function.

The amplitude, mean, and variance of the lognormal distribution can be inferred from the parameters a, b, and c in a straightforward manner, the results of which are given below:

$$\sigma = \frac{1}{\sqrt{-2a}}$$

$$\ln \nu_0 = \sigma^2(1+b)$$

$$\ln A = c + \frac{(\ln \nu_0)^2}{2\sigma^2} + \frac{1}{2}\ln(2\pi\sigma^2)$$

Using least-square methods, the log of the raw data can, therefore, be easily fit to a polynomial to determine the mean and variance of the lognormal distribution. This technique eliminates the need

to take several partial derivatives of the lognormal distribution and simplifies the fitting algorithm. The fit is shown along with the original data in Fig. 5. Data points near saturation and data points around the minimum signal level resulting from pointing errors were not considered. The resulting fit had a mean of $\nu_0 = 1.81$ V and $\sigma^2 = 0.49$. These numbers account for contributions from both scintillation and beam motion/jitter. In the presence of multiple beams, it is more convenient to use the actual mean and standard deviation of the distribution as opposed to indirect measures such as log-variance. From $\ln < V >= 0.5\sigma^2 + \ln v_0$, we find that the mean of the fit is $< V >= 2.3$ V. It is also useful to define a normalized standard deviation, $SD = (< V^2 > - < V >^2)^{1/2} / < V >$ for the distribution. It is easy to show that $SD = (\exp(\sigma^2) - 1)^{1/2}$, and therefore the standard deviation is 0.80 for the fit.

V. Comparison of Theory and Experiment

Figure 6 shows the predicted (with one and two beams) and experimentally observed pdf's for the QPD signal. Figure 6 also lists the mean and standard deviation for each of the theoretical and experimental curves. For two beams, the theory predicts the standard deviation of the signal to be 0.71, while it is 0.80 for the experimental fit. The difference arises mainly from the uncertainty in the transmitter pointing jitter and the unaccounted satellite tracking errors (discussed later). The electronics on board the satellite are susceptible to Earth's radiation belts, and the resulting noise can increase signal variation as well. Additional data from the planned experiments with a single uplink beam will enable better comparison to theory.

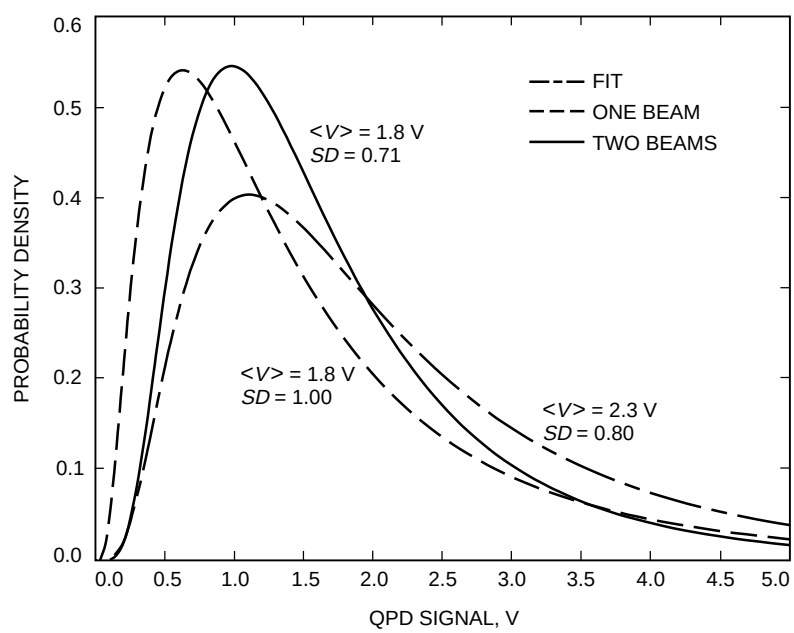

Fig. 6. Expected and observed pdf of the QPD signal, showing the experimental lognormal fit of Fig. 5, the theoretical pdf for a single uplink beam, and the expected pdf in the presence of two uplink beams.

The discrepancy between the predicted and observed mean values, on the other hand, is just over 1.5 dB. It is interesting to note that the theoretical and observed most-likely value of the QPD voltage reading is almost identical. The agreement between theory and experiment for the mean value is surprisingly good given the various unknown factors that are currently being investigated. Recent experiments suggest a reduction in the sensitivity of the detector with time due to temperature increases. The effect of excessive exposure to Earth's radiation belts on the QPD and charge-coupled device (CCD) sensitivity is

still unclear. Some of the difference can be attributed to uncertainties in the optical loss of the transmitter system, which was estimated from the number of elements in the optical train. Also, the atmospheric transmission value at the uplink wavelength needs to be updated from the planned recalibration of the atmospheric visibility monitoring (AVM) data. Moreover, neither the transmitter pointing offset nor the beam divergence is accurately known.

As is apparent from Fig. 4, there is a slow (on the order of minutes) decay in the signal level followed by a sharp jump to a high value. This is due to drift in the tracking of the beacon by the satellite, which is not included in the analysis. The tracking errors cause the out-of-focus beam to fall partially outside the area of the QPD and, hence, cause a reduction in the detected signal. The slow decays in received signal power partly explain the large variance in the observed signal. Faster sampling of the beacon signal from the communication detector should provide additional data about temporal statistics of scintillation. Downlink signal statistics will provide information on satellite vibrations, pointing accuracy, and pointing drift that will further enable us to better isolate atmospheric scintillation effects.

Acknowledgments

The authors wish to thank the members of the GOLD team and the scientists at the Communications Research Laboratory who were involved in the experiments for their cooperation.

References

[1] J. W. Goodman, *Statistical Optics*, New York: John Wiley and Sons, 1985.

[2] R. E. Hufnagel, "Variations of Atmospheric Turbulence," *Digest of Topical Meeting on Optical Propagation Through Turbulence*, Paper WA1, Optical Society of America, Washington, DC, 1974.

[3] G. C. Valley, "Isoplanatic Degradation of Tilt Correction and Short-Term Imaging Systems," *Appl. Opt.*, vol. 19, 1980.

[4] F. G. Smith, ed., *Atmospheric Propagation of Radiation*, vol. 2, Bellingham, Washington: SPIE Optical Engineering Press, 1993.

[5] W. L. Wolfe and G. J. Zissis, eds., *The Infrared Handbook*, revised edition, Ann Arbor, Michigan: Environmental Research Institute of Michigan, 1989.

[6] K. Kiesaleh and T.-Y. Yan, "A Statistical Model for Evaluating GOPEX Uplink Performance," *The Telecommunications and Data Acquisition Progress Report 42-111, July–September 1992*, Jet Propulsion Laboratory, Pasadena, California, pp. 325–332, November 15, 1992.

[7] L. C. Andrews and R. L. Phillips, "I-K Distribution as a Universal Propagation Model of Laser Beams in Atmospheric Turbulence," *Journal of the Optical Society of America*, vol. 2, pp. 160–163, 1985.

[8] L. C. Andrews, R. L. Phillips, and B. K. Shivamogg, "Relations of the Parameters of the I-K Distribution for Irradiance Fluctuations to Physical Parameters of the Turbulence," *Appl. Opt.*, vol. 27, pp. 2150–2156, 1985.

[9] V. I. Tatarskii, *Wave Propagation in Turbulent Medium*, New York: McGraw-Hill, 1961.

[10] A. Ishimaru, *Wave Propagation and Scattering in Random Media*, vol. 2, New York: Academic Press, 1978.

[11] S. F. Clifford, G. R. Ochs, and R. S. Lawrence, "Saturation of Optical Scintillation by Strong Turbulence," *Journal of the Optical Society of America*, vol. 64, no. 148, 1974.

[12] K. Kiesaleh, "On the Probability Density Function of Signal Intensity in Free-Space Optical Communications Systems Impaired by Pointing Jitter and Turbulence," *Opt. Eng.*, vol. 33, pp. 3748–3757, 1994.